Structural Monitoring and Maintenance, *Vol. 2, No. 2 (2015) 145-164*
DOI: http://dx.doi.org/10.12989/smm.2015.2.2.145

Monitoring bridge scour using dissolved oxygen probes

Faezeh Azhari[1a], Peter J. Scheel[2b] and Kenneth J. Loh[*1]

[1]*Department of Civil & Environmental Engineering, University of California, Davis, CA 95616, USA*
[2]*Department of Mechanical & Aerospace Engineering, University of California, Davis, CA 95616, USA*

(Received January 16, 2014, Revised March 23, 2015, Accepted May 9, 2015)

Abstract. Bridge scour is the predominant cause of overwater bridge failures in North America and around the world. Several sensing systems have been developed over the years to detect the extent of scour so that preventative actions can be performed in a timely manner. These sensing systems have drawbacks, such as signal inaccuracy and discontinuity, installation difficulty, and high cost. Therefore, attempts to develop more efficient monitoring schemes continue. In this study, the viability of using optical dissolved oxygen (DO) probes for monitoring scour depths was explored. DO levels are very low in streambed sediments, as compared to the standard level of oxygen in flowing water. Therefore, scour depths can be determined by installing sensors to monitor DO levels at various depths along the buried length of a bridge pier or abutment. The measured DO is negligible when a sensor is buried but would increase significantly once scour occurs and exposes the sensor to flowing water. A set of experiments was conducted in which four dissolved oxygen probes were embedded at different soil depths in the vicinity of a mock bridge pier inside a laboratory flume simulating scour conditions. The results confirmed that DO levels jumped drastically when sensors became exposed during scour hole evolution, thereby providing discrete measurements of the maximum scour depth. Moreover, the DO probes could detect any subsequent refilling of the scour hole through the deposition of sediments. The effect of soil permeability on the sensing response time was also investigated.

Keywords: bridge; dissolved oxygen optode; flood; hydraulic structures; scour; structural health monitoring

1. Introduction

Flowing water, especially during floods, erodes the soil around bridge piers and abutments through current-induced horseshoe and wake vortices (Dargahi 1990, De Falco and Mele 2002). This phenomenon, referred to as scour, decreases the axial and lateral capacity of the bridge supports and can lead to undesirable deflections, structural instability, or even failure. During the 1987 spring floods, for instance, scour was responsible for the damage or failure of 17 bridges throughout New York and the New England area in the U.S. (White 1992).

A recent example of scour-induced bridge failure occurred as a result of the June 2013 flood

∗Corresponding author, Associate Professor, E-mail: kjloh@ucdavis.edu
[a] Ph.D. Candidate, E-mail: fazhari@ucdavis.edu
[b] B.Sc., E-mail: peter.j.scheel@gmail.com

http://www.techno-press.org/?journal=smm&subpage=7 ISSN: 2288-6605 (Print), 2288-6613 (Online)

event in Calgary, Canada, where the Bonnybrook Bridge sagged at one of the four bridge piers and caused a train carrying petroleum distillate to derail (Wingrove 2013). Emergency measures were taken to pump out the flammable fluids and to prevent the railcars from falling into the swollen Bow River. This potentially disastrous incident was not a rare event. In fact, bridge scour is the predominant source of overwater bridge failures around the world (Butch 1996, Hong *et al.* 2012, Parsons *et al*. 2014).

In fact, bridge scour is not a modern day engineering problem but rather has been an issue that has been recognized for centuries. In his 1856 publication, Joseph Minard, a French engineer and bridge inspector, provided descriptive drawings depicting bridge scour failures (see Fig. 1 for two examples). His account of scour conditions was aimed at demonstrating the prevalence of upstream scour in flood-induced bridge failures (Minard 1856). This assertion could also be inferred from a study by Butch (1996) on over 120 bridge piers in New York, where the deepest part of the scour holes was shown to commonly be on the upstream side at a distance of less than one pier width. Thus, to achieve suitable design procedures or remediation strategies, it would be wise to seek potential scour depths, at least, at the upstream.

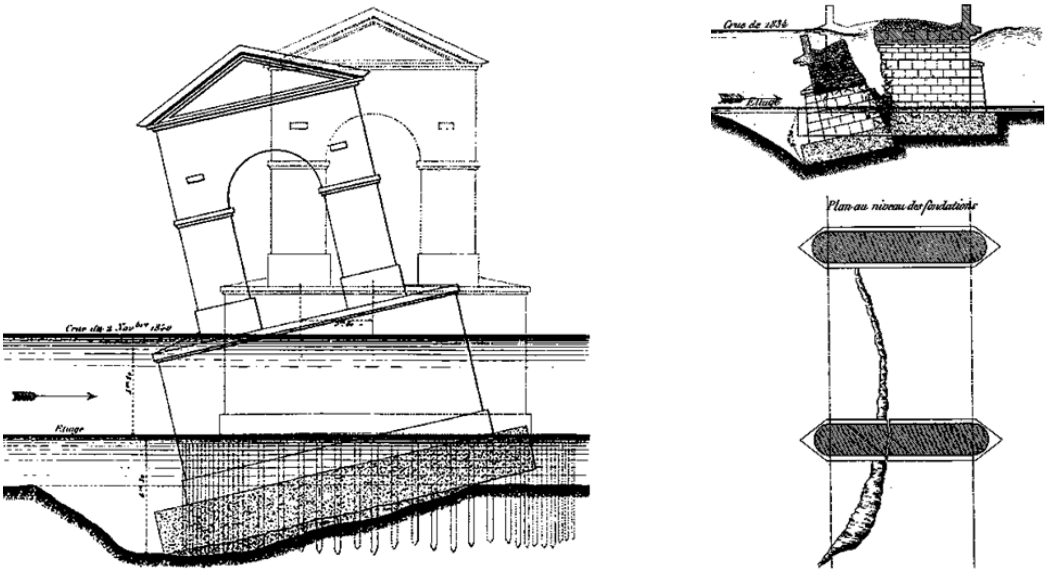

(a) (b)

Extracted from De la chute des ponts dans les grandes crues by Minard, published in Paris, in 1856 (Collections de l'École nationale des ponts et chaussées). Image provided courtesy of École des Ponts ParisTech.

Fig. 1 Scour-induced failures at two bridges in France are depicted: (a) Bourg-Saint-Andéol Bridge on the Rhône River during the flood of 1840, where a 4 m-deep scour caused the entire pier to tilt and advance 3.8 m upstream; (b) Coise Bridge on the Coise department of Loire during the flood of 1834, where a maximum scour depth of 3.3 m split a pier into two parts, one of which collapsed into the scour hole [12]

The extent and shape of a scour hole depends on a slew of factors including, but not limited to: approach flow velocity, pier or abutment geometry, bed sediment shape and type, water depth, and pile group arrangements (Allen 1965, Melville and Raudkivi 1996, Apsilidis *et al.* 2010, Deng and Cai 2010). One can estimate maximum scour depths through artificial neural networks (Choi and Cheong 2006), numerical modeling (Sumer 2007), and empirical equations (Johnson 1995; Benedict *et al*. 2007). These methods, however, are only predictive and typically not inclusive of all situations. Because of these models' limited predictive capabilities, scour monitoring becomes imperative for detecting conditions that may jeopardize structural safety.

To date, visual methods, including intermittent inspections and measurements completed by trained divers, are one of the predominant methods used to survey scour-prone bridge piers. These measurements, although relatively accurate, are inherently sporadic and are often not conducted at the critical time of maximum scour. Moreover, during flood events, turbulent and murky waters make routine visual inspections by divers almost impossible and extremely unsafe, as was the case in the Bonnybrook Bridge scour incident (Wingrove 2013).

Therefore, an automatic real-time monitoring system needs to be employed to detect the onset and extent of scour and to inform the authorities in a timely manner so that appropriate measures can be taken to ensure bridge integrity and public safety. Transportation agencies and bridge owners use an eclectic range of technologies for bridge scour monitoring, including magnetic collar (Richardson et al. 1996), sonar (De Falco and Mele 2002), radar (Millard *et al*. 1998, Park *et al.* 2004), time-domain reflectometry (TDR) (Yankielun and Zabilansky 1999, Yu and Zabilansky 2010), float-out devices (Lueker *et al*. 2010), fiber optics (Lin *et al.* 2005), and tilt sensors (Yao *et al.* 2010, Briaud *et al*. 2011). The challenges associated with these sensors include their large size, low resolution, low reliability, costly and difficult installation procedures, vulnerability to debris, and tedious post-processing requirements (Hunt 2005, Deng and Cai 2010, Yu and Yu 2010, Zhou *et al*. 2011), to name a few.

Recent research, directed towards eliminating the aforementioned shortcomings, has led to the development of several innovative scour sensing devices. Digital switch sensors (Liu *et al*. 2010), enhanced fiber optic sensors (Xiong *et al*. 2012), micro-electromechanical systems (MEMS) (Lin *et al*. 2010), smart rocks (Chen *et al*. 2012), erosion function apparatus (EFA) (Briaud *et al.* 2001), and piezoelectric sensors (Azhari *et al*. 2014) are examples of these research prototypes. While these technologies each purport to improve the scour monitoring procedure, they involve intricate designs and suffer from certain limitations, such as lack of mechanical robustness, extensive post-processing requirements, and susceptibility to hydrostatic and soil pressure. In this study, a more straightforward scour monitoring system is introduced, where dissolved oxygen (DO) optodes are the sensing devices.

In September 2000, the DO readings in a Washington State river fell to less than 1 mg/L from its standard level of 8 mg/L. After assessing various factors affecting oxygen concentration, Ebbert *et al*. (2002) concluded that bed sediments inundating DO sensors was almost certainly the reason for the observed hypoxia. The work presented in this paper was instigated by this finding, as well as other relevant ones identifying low DO levels caused by the intrusion of finer sediments in the spawning gravels (Koski 1966, Shirazi and Seim 1981, Kondolf *et al.* 2008), which was among factors that triggered salmonid embryo mortality. According to these findings, oxygen is depleted in riverbed sediments (perhaps due to metabolic processes). In this case, scour is a result of the excavation and removal of sediments by flowing water, which has much higher oxygen levels. Therefore, oxygen-triggered sensors can potentially be used to determine scour depths.

Fig. 2 Fiber optic DO dipping probes were used as scour sensing devices

In this study, the viability of monitoring scour via DO measurements at various depths in the streambed surrounding a bridge pier or abutment was explored. The premise of this sensing scheme is that, while the sensors are embedded in soil, the dissolved oxygen levels are negligible. However, once scour occurs and exposes a sensor, the oxygen levels would increase significantly and reach the flowing water DO level. Thus, by monitoring oxygen levels at sensor locations, one could deduce scour depth. Following preliminary proof-of-concept tests, a set of experiments was conducted in which DO probes were embedded at different soil depths inside a laboratory flume simulating local scour conditions. This paper begins with a description of a commercial DO sensing system used in this study. Next, the experimental setup and sensor instrumentation layout are discussed. Experiments were conducted in a laboratory flume, where four DO probes were installed (facing upstream) along the buried length of a circular pier. The results from extensive laboratory tests are then presented, as well as the different sensor responses observed corresponding to different soil conditions tested and the effects of scour hole refill. The use and advantages of DO sensors are also compared to other existing and emerging technologies employed for scour monitoring. Finally, the paper concludes with a brief summary of major findings and future research opportunities.

2. Background and experimental details

2.1 DO Sensors

Fiber optic oxygen dipping probes DP-PSt3 (Fig. 2), acquired from PreSens Precision Sensing GmbH, were chosen primarily for their small size and mechanical robustness. With an outside diameter of only 4 mm, these sensors did not affect flow conditions and can be housed in a compact conduit attached to a bridge pier or abutment. Also, unlike DO sensors that utilize electrolyte solutions, solution replenishing or membrane cleaning and replacement are not an issue with these optical sensors. The DO probes have no cross-sensitivity with pH, ionic species, electrical interferences, or magnetic fields. They are polarization-free, pressure resistant, and offer

long-term stability, which means that they can be embedded in soil for a long period (Klimant and Meyer 1995), consistent with typical bridge scour monitoring needs. DO is, however, dependent on temperature, and therefore temperature corrections may be necessary as discussed in later sections.

As shown in Fig. 2, the optical oxygen sensor (optode) comprises of a polymer optical fiber with a thin coat of oxygen-sensitive luminophore at its distal tip. The sensing and measurement mechanism is based on the principle of dynamic luminescence quenching by oxygen (Klimant and Meyer 1995), as described in Fig. 3. A light-emitting diode (LED) excites the sensor, normally causing the sensor spot to emit luminescence; however, in the presence of oxygen, the indicator molecule transfers energy to the oxygen molecule through a collision, which would result in the quenching of the measurable luminescence signal (Klimant *et al*. 1997). The signal is then delivered via the optical fiber, which is connected to a computer-controlled transmitter. The transmitter uses a phase modulation technique to evaluate the DO content. The measured phase angle between the exciting and emitted sinusoidal signals, ϕ, is related to the luminescence decay time of the luminophore, τ

$$\tan\phi = 2\pi\, f_{\mathrm{mod}}\, \tau \tag{1}$$

where f_{mod} is the modulation frequency (John and Huber 2005). The decay time and the fluorescence intensity, I, could in turn be expressed as a function of the oxygen content, $[O_2]$, through the Stern-Volmer equation (Stern and Volmer 1919); therefore

$$\frac{\tan\phi_0}{\tan\phi} = \frac{\tau_0}{\tau} = \frac{I_0}{I} = 1 + K_{sv}[\mathrm{O}_2] \tag{2}$$

where ϕ_0, τ_0, and I_0 are the phase angle, decay time, and intensity, respectively, in the absence of oxygen, and K_{sv} is the Stern-Volmer constant. More information on dynamic luminescence quenching, optode oxygen sensors, and the dependence of phase shift on oxygen concentration can be found in other published studies (Klimant and Wolfbeis 1995, Klimant *et al.* 1997). The DO probes used in this study had a measurement range of 0 to 45 mg/L and a resolution of ±0.005 to ±0.025 mg/L (i.e., depending on DO levels).

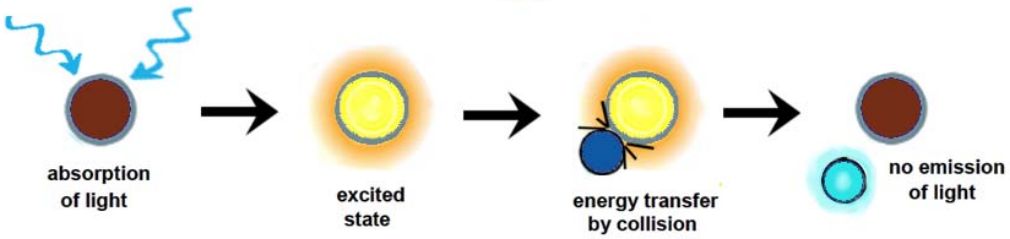

Fig. 3 The principle of dynamic (or collisional) quenching of luminescence by oxygen is shown. Molecular oxygen deactivates the luminescence procedure, which would have occurred in the absence of oxygen (adapted from [57]).

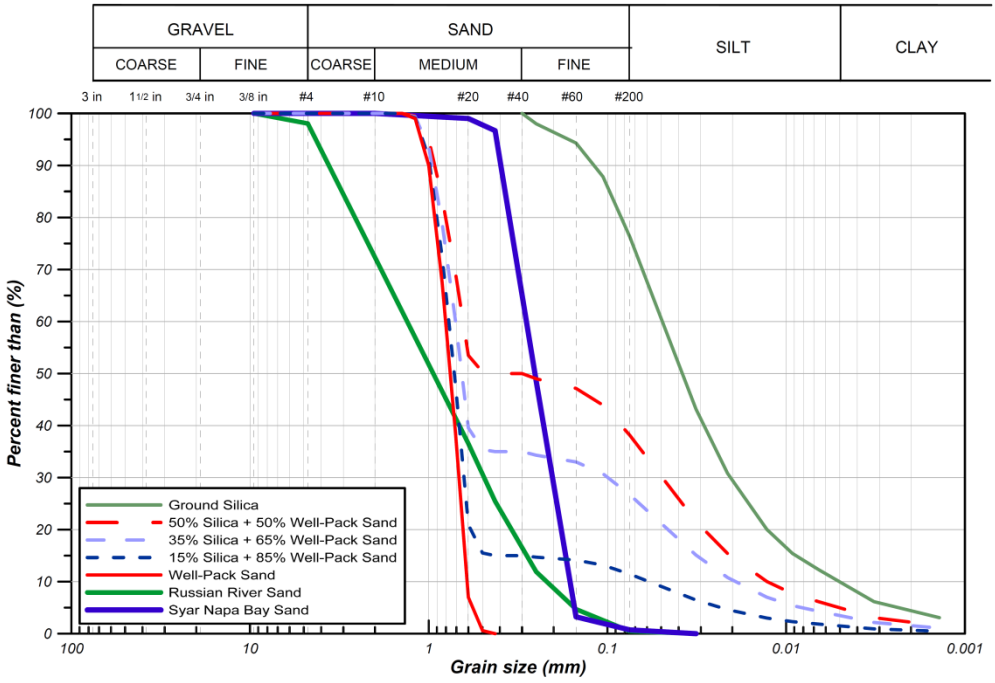

Fig. 4 Soil grain size distribution curves based on the unified soil classification system (USCS), ASTM standard D2487 (2011)

2.2 Soil gradations and properties

Scour initiation and evolution is a function of the riverbed material type, shape, and size, in addition to the nature of the flow (Allen 1965, Melville and Coleman 2000, Govindasamy *et al.* 2013). Furthermore, one of the main factors influencing DO concentrations in bed sediments is hydraulic permeability (Dat *et al.* 2004, Precht *et al.* 2004), which is a function of the soil gradation. Therefore, to account for the sediment type dependence, experiments were conducted using six different soil mixtures. The particles' size distributions, presented in Fig. 4, were obtained by dry sieving the soils according to ASTM D421-85 (2007).

Soil permeability values presented in Table 1 were estimated using Hazen's empirical formula (Hazen 1892, Hazen 1911), which is commonly used for saturated sandy soils

$$k = C(D_{10})^2 \tag{3}$$

where k is the coefficient of permeability (cm/s), C is Hazen's empirical coefficient (assumed to be its average value of 1.0), and D_{10} is the effective grain size (in mm) for which 10% of the soil is finer. As a reference, Table 2 provides typical values of k for soils with various degrees of permeability. Also, by analyzing pooled data from 41 different rivers around the world, Calver (2001) reported riverbed permeability to range predominantly from 10^{-5} to 10^{-1} cm/s. According to these references, the soil types tested in this research cover a wide range of permeability from very low to high values and represent a reasonable portion of expected riverbed materials.

Table 1 Soil properties

Test	Bed Soil Type	D10 [mm]	D50 [mm]	D90 [mm]	k [cm/s]	Ucr [m/s]
1	Well-Pack Sand: #20 WS (from Red Flint Sand & Gravel, LLC.)	0.610	0.75	1	$3.7 \times 10_{+}$	0.329
-	Ground Silica: SIL-CO-SIL® 250* (from U.S. Silica Company)	0.005	0.027	0.113	2.5×10^{-5}	-
2	15% Silica + 85% Well-Pack Sand	0.075	0.715	0.97	5.6×10^{-3}	0.321
3	35% Silica + 65% Well-Pack Sand	0.021	0.63	0.97	4.5×10^{-4}	0.298
4	50% Silica + 50% Well-Pack Sand	0.013	0.3	0.91	1.6×10^{-4}	0.249
5	Syar Napa Bay Sand	0.15	0.25	0.4	2.3×10^{-2}	0.274
6	Russian River Sand	0.22	0.93	3.5	4.8×10^{-2}	0.304

*The information for ground silica is provided as a reference

Table 2 Typical degrees of permeability

Degree of Permeability	Soil Type	k [cm/s]
High	Clean gravels and clean sands	$> 10^{-1}$
Medium	Clean sand and gravel mixtures	10^{-3} to 10^{-1}
Low	Very fine sands and Mixtures of sand, silt and clay	10^{-5} to 10^{-3}
Impermeable	Unfissured clays and clay-silts	10^{-9} to 10^{-5}

2.3 Flume setup

A 7.3 m-long, clear acrylic laboratory flume with a rectangular cross-section (45.7 cm wide and 61 cm deep) was used in this study. An acrylic cylinder (7.62 cm in diameter) was placed in the middle of the flume to simulate a bridge pier and to house the DO sensors as illustrated in Fig. 5. It can be seen from Fig. 5 that the instrumentation layout was such that S1 was closest to the surface, and S4 was buried the deepest. Boxes spanning the entire width of the flume were placed upstream and downstream of the pier such that the gap between the boxes was approximately 3.7 m. This gap was filled with a 30 cm-deep layer of clean and uniformly graded well-pack sand (*i.e.,* Test #1 of Table 1). To straighten the flow, a series of 50 cm-long pipes were affixed to the upstream box.

For experiments conducted using the other five soil types (i.e., Tests #2 to #6 of Table 1), a 15.2 cm-diameter cylindrical mold was used to place a column of that soil around the pier in the fashion shown in Fig. 6. This method had two advantages: first, there was no need to replace over 0.5 m^3 of soil for each test; second, the clean sand, used as the base material, did not murk the water during flow and allowed for accurate observational measurements during the experiments.

2.4 Sensor instrumentation and experimental procedure

Four DO probes were mounted along the pier at 5 cm, 9 cm, 11 cm, and 20 cm depths below the initial soil level (see Fig. 5) by inserting them into the predrilled holes in the cylinder and securing the tips using rubber washers. The sensors were connected to the OXY-4 mini, a

four-channel fiber optic oxygen transmitter, and the system was connected to a computer that was controlled by the software OXY4v2_30FB from PreSens Precision Sensing GmbH. The sensors were then calibrated using the pressure, temperature, and phase values provided in the accompanying data sheets. Measurement rates were set to the maximum available frequency, which was 0.2 Hz.

The soil surface was smoothed and leveled using a trowel before slowly being saturated. Then, the flow rate was increased slightly to less than 0.1 m/s. At this low flow rate, erosion could not occur, yet water was not stagnant either. Depending on soil permeability, some pore water flow was possible. DO levels were monitored for some time until the values dropped well below the control water DO level. It should be mentioned that not all of the experiments were left to reach their absolute minimum DO levels or 0 mg/L before scour tests were commenced. However, this was not an issue since the concept of this sensing technique was based on DO measurement discontinuities and for it to reach the DO level of the surrounding flowing water. It should be mentioned that, prior to each experiment, one of the sensors was placed above the soil level, and the flowing water DO level was recorded for reference.

To start the actual scour tests, the flow rate was increased to the maximum allowed by the flume geometry, considering the 30 cm layer of soil. The velocity profile, presented in Fig. 7, was measured using a FlowTracker Handheld Acoustic Doppler Velocimeter (ADV) from SonTek/YSI. The mean flow velocity was 0.35 m/s, which was larger than the mean critical velocity ($\overline{U}_{cr}$) calculated for all soil types (see Table 1) and thus was adequate for the initiation of live-bed scour. $\overline{U}_{cr}$ is the depth averaged threshold speed above which motion initiated and sediment transport occurred and was estimated using van Rijn's formulae (van Rijn 1984, Soulsby 1997):

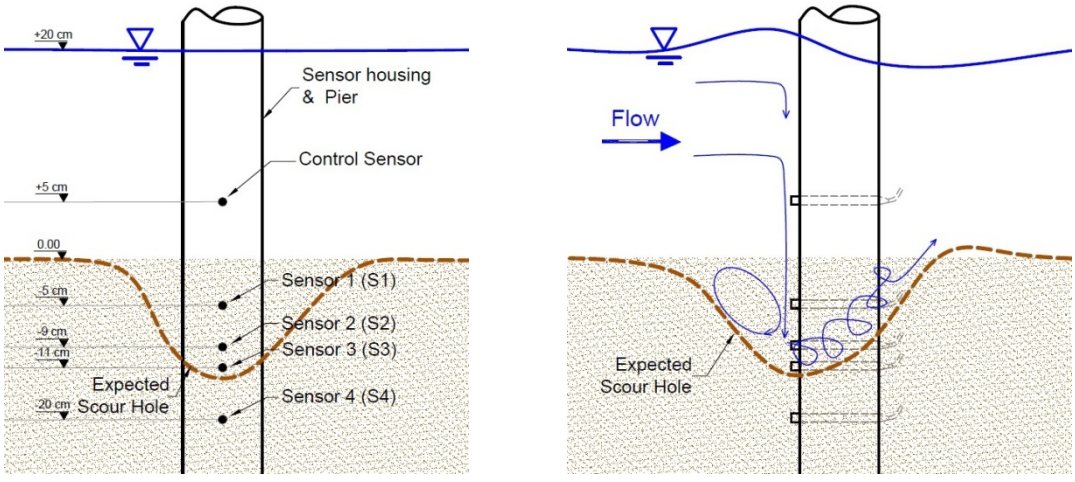

(a) (b)

Fig. 5 DO sensor arrangement: (a) view facing the flow and (b) side view

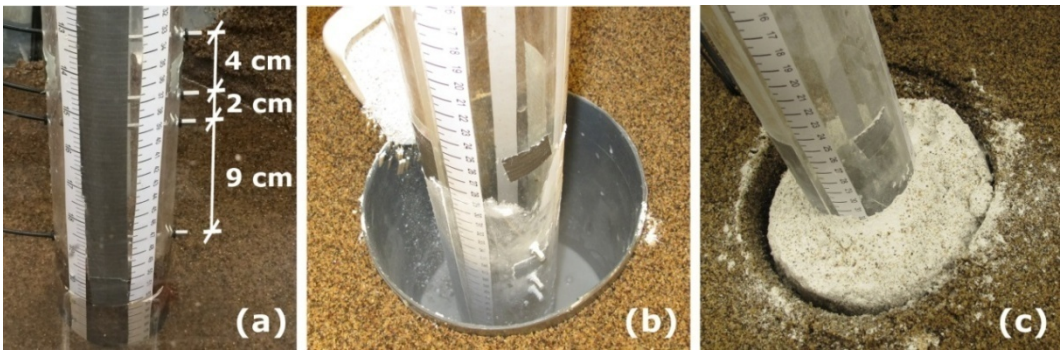

Fig. 6 Sediment filling process: (a) sand surrounding the pile was removed; (b) a cylindrical tube was placed around the pier, sand was backfilled against it, and the soil being tested was poured gradually to prevent segregation; (c) the cylinder was removed, the interface was smoothed, and the soil surface was leveled

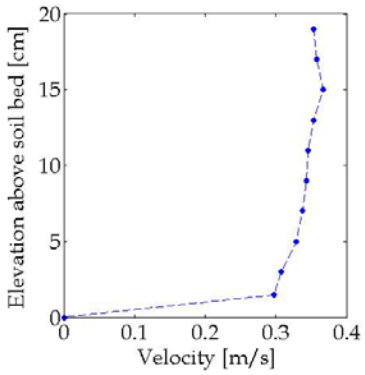

Fig. 7 Velocity profile

$$\overline{U}_{cr} = 0.19(D_{50})^{0.1} \log_{10}(4h/D_{90}) \quad \text{for} \quad 100 \le D_{50} \le 500\,\mu m \tag{4}$$

$$\overline{U}_{cr} = 8350(D_{50})^{0.6} \log_{10}(4h/D_{90}) \quad \text{for} \quad 5100 \le D_{50} \le 2000\,\mu m \tag{5}$$

where h is the water depth, and D_{50} and D_{90} are the grain sizes for which 50% and 90%, respectively, of the soil is finer. The units used for all the variables in Eqs. (4) and (5) are in meters and seconds.

The scour hole around the cylindrical pier increased in size and depth with time, consecutively exposing DO sensors S1, S2, and S3. The maximum scour depth was visually inspected (using the gradations on the side of the cylinder) and recorded at various times during scour development. The flow rate was decreased at a maximum scour depth of ~13 cm such that S4 remained buried. Fig. 8 shows a picture taken during scour hole development when S1 and S2 were completely exposed and when S3 was only partially exposed.

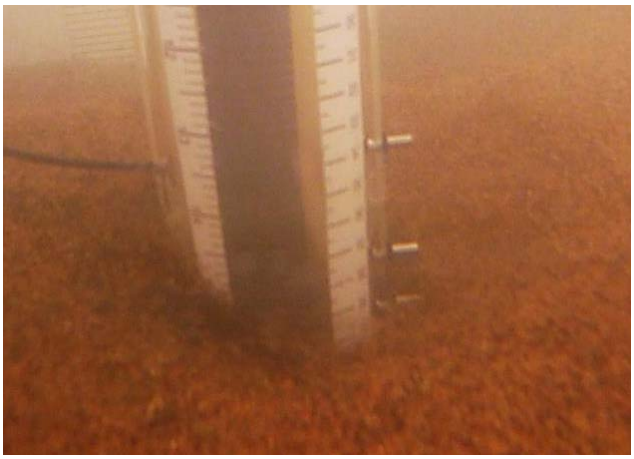

Fig. 8 A snapshot during the scour hole development, where S1 and S2 were completely exposed, while S3 was partially exposed

2.5 Temperature dependence

DO is strongly influenced by water temperature (Glud 2008; Kondolf et al. 2008), decreasing as the temperature increases; therefore, it was important that temperature variations be included in the calibration process. In fact, in a preliminary experiment that was performed as a proof-of-concept, the Fibox 3 transmitter from PreSens was used, in which temperature compensation was done automatically through a precision temperature sensor that was embedded in the soil alongside the DO sensor. The Fibox 3, however, could only accommodate one DO sensor.

Since the OXY-4 mini did not contain temperature sensors, the laboratory ambient temperature of 23°C was used in the data acquisition software for all the tests. Water temperature was measured and recorded intermittently using a thermometer. These values were then used to perform temperature corrections as described in this section. In the experiments presented in this study, although water temperatures varied from one test to the other, they did not change during each single scour test due to their short duration. After each experiment, DO values were corrected using the recorded temperature. The following calibration relations, obtained by linear regression of ϕ_0 and K_{sv} values obtained at various temperatures, were used (John and Huber 2005)

$$\phi_0 = 62.14 - 0.08915\,T \tag{6}$$

$$K_{sv} = 0.04899 - 4.965\times10^{-4}\,T \tag{7}$$

where ϕ_0 and K_{sv} are the phase angle and Stern-Volmer constant, respectively, used in Eq. (2) for calculating DO contents. T is the temperature for each experiment in °C.

For verification purposes, a simple test was conducted in which a single DO probe was used to measure oxygen content in water (taken from the flume) at various temperatures ranging from 4 to

50°C. These measurements were compared against DO values calculated using an empirical equation (John and Huber 2005), which estimated oxygen solubility (mg/L) in air-saturated fresh water as a function of temperature, pressure, and humidity

$$DO = \frac{p_{atm} - p_w}{p_N} y_{0_2} \alpha \frac{M_{O_2}}{V_M} \tag{8}$$

where P_{atm} is 1,012.5 mbar (i.e., atmospheric pressure at the experimental site in Davis, CA, USA), P_N is the standard pressure (1,013 mbar), y_{O2} or the mole fraction of oxygen in air is 0.2095, M_{O2} is the molecular mass of oxygen (32g/mol), and V_M is the molar volume (22.414 mol/L). It should be noted that P_w, water vapor pressure, and α, the Bunsen absorption coefficient, are both temperature-dependent (John and Huber 2005)

$$p_w = \exp\left(52.57 - \frac{6690.9}{T} - 4.681 \ln T\right) \tag{9}$$

$$\alpha = 10^{-3} \exp\left(\frac{8553}{T} + 23.78 \ln T - 160.8\right) \tag{10}$$

where T is the temperature in °K.

As shown in Fig. 9, the DO values measured using the probe followed the empirical relation trend closely. The observed differences were perhaps due to the fact that the flume water conditions were slightly different than those of fresh water. For example, the effect of water salinity (John and Huber 2005, Kondolf *et al*. 2008) on DO may be a factor responsible for this deviation shown in Fig. 9.

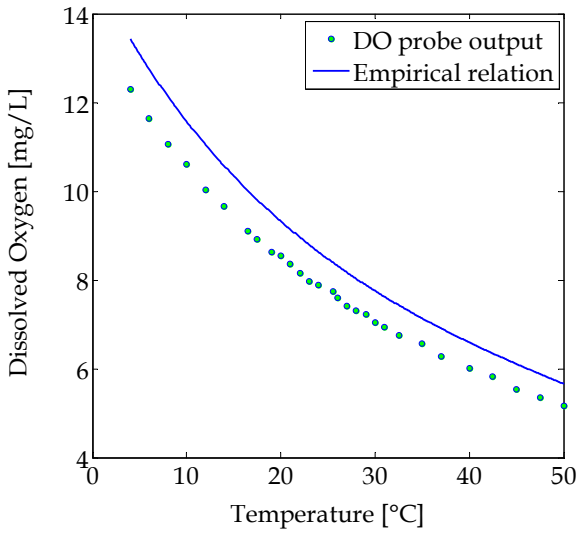

Fig. 9 Effect of water temperature on DO content

3. Results and discussions

3.1 DO sensing for scour monitoring

Scour tests were performed for the six different soil materials as described in Section 2.3. Fig. 10 shows a representative set of results for scour testing conducted using "35% Silica + 65% Well-Pack Sand" soil mixture (i.e., Test #3 of Table 1). Here, the DO time histories for all four sensors are overlaid with the progression of scour, as illustrated by the scoured soil profile (with reference to the right-hand-side vertical axis of Fig. 10) showing soil levels at the simulated pier. Soil level was initially zero prior to the initiation of scour and at time zero and then gradually decreased to 11.2 cm below the original level. In addition, Fig. 10 also shows three sets of circles representing the four sensors. The placement of these circles correspond to when different sensors became exposed due to scour, which corresponded to 4, 25, and 53 min for sensors S1, S2, and S3, respectively; S4 remained buried throughout the experiment. The dark circles in Fig. 10 denote buried sensors that were not exposed to water at that instant (e.g., S4 for the entire duration of the test shown in Fig. 10), whereas open circles denote exposed conditions.

Fig. 10 shows the DO level variation for each sensor according to the provided legend. DO values were at their minimum value of 0 when the sensor was unaffected by scour but increased to that of the flowing water DO level once soil was removed due to scour. During this particular experiment, the water temperature was 29°C, and the water DO level was at 7.2 mg/L (i.e., represented by a black horizontal line in Fig. 10). As evident from the data shown in Fig. 10, the DO sensors provided a clear indication of scour; maximum scour depth could be estimated based on the depth of exposed sensors measuring DO levels as high as the water DO.

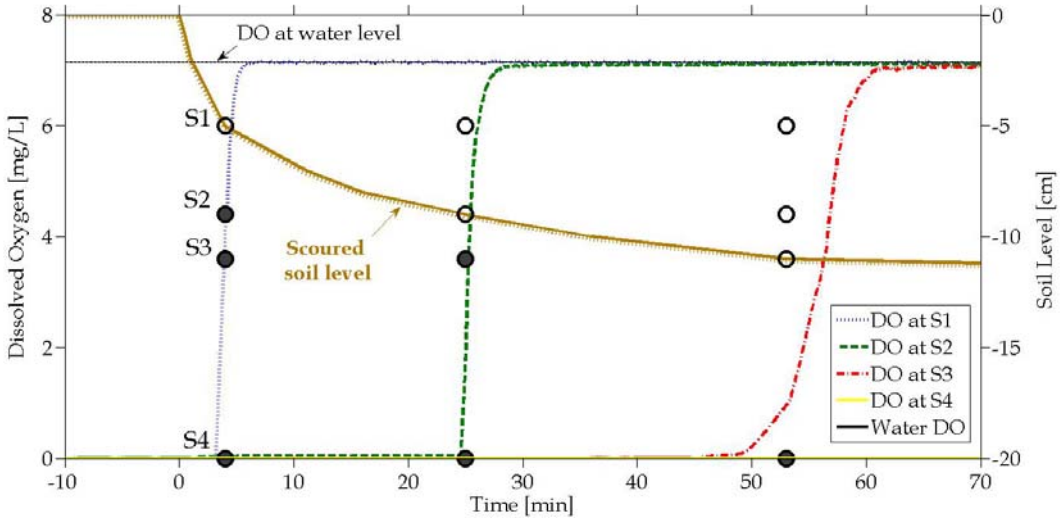

Fig. 10 Scour sensing results for the "35% Silica + 65% Well-Pack Sand" soil type are presented. The filled and open circles symbolize buried and exposed DO probes, respectively.

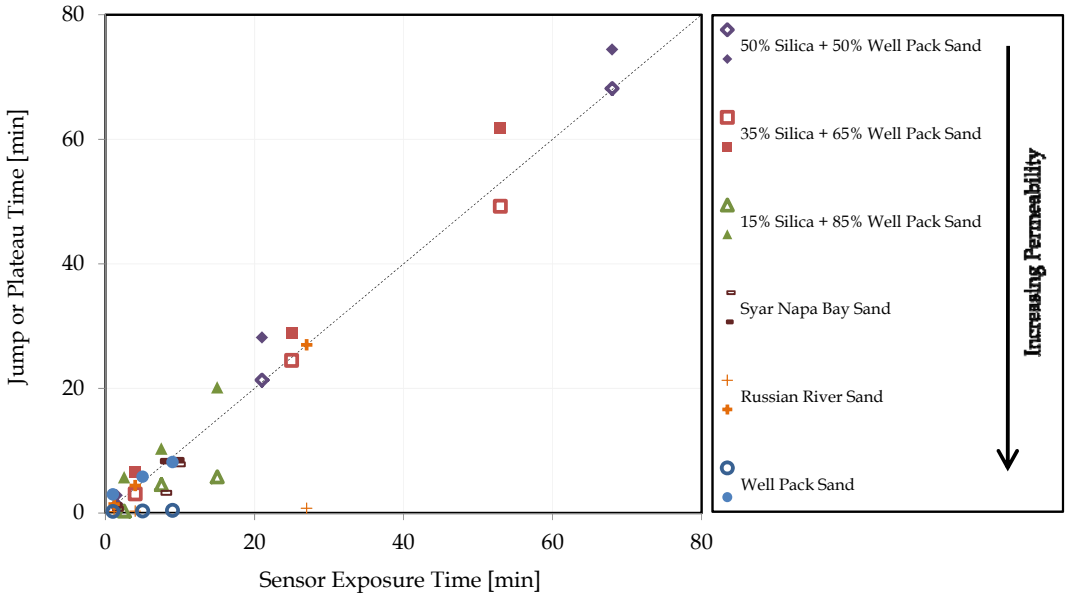

Fig. 11 The DO jump and plateau times were compared with the time at which the sensor tip was visually observed (i.e., when the scour hole reached the buried sensor). Hollow symbols denote signal jump, whereas filled ones represent the start of signal plateau

3.2 Effects of soil permeability

Depending on the soil material, the increase in DO levels occurred at different rates. The test results presented in Fig. 10 correspond to a low permeability soil for which the upsurge in DO levels and sensor exposure occurred almost simultaneously. This was not the case for all soil types; for highly permeable soils, the sensors emerged from the soil only after the DO measurement plateaued to that of the ambient flowing water DO level (i.e., the steady-state value). Thus, to quantify these differences, two time recordings were also made for each sensor, namely when DO signal started to increase (or jump), and the time at which it reached the water DO level and plateaued thereafter. In addition, the time it took from the start of the test to each sensor emerging from under the sediment (due to scour) was also recorded and was defined as sensor exposure time. Fig. 11 presents a summary of the scour test results from all six soil types by comparing the signal jump (denoted with open symbols) and plateau initiation times (indicated with filled symbols) with the observed sensor exposure times. The values presented in Fig. 11 are also tabulated in Table 3.

The results indicate that, first of all, soils with higher permeability scoured much faster because of their looser nature, whereas it took the less permeable and more densely packed soils much longer to scour to soil levels beneath S3. Second, for the less permeable soils, the jump and plateau times were both close to the time at which the sensor emerged from under the sediments and the sensor tip was visually observed. As permeability increased, however, only the plateau times show values close to the observed exposure times.

Table 3 Sensor jump, plateau, and observed times for different soil types tested

Soil Type (see Table 1)	#1	#2	#3	#4	#5	#6
Permeability k [cm/s]	3.6E-01	5.6E-03	4.5E-04	1.6E-04	2.3E-02	4.8E-02
S1 Jump*	0.25	0.33	3.08	1.17	0.67	0.2
S1 Plateau	2.98	5.75	6.5	2.83	1.25	1.41
S1 Observed	1	2.5	4	1.5	1	1.16
S2 Jump	0.33	4.58	24.5	21.33	3.25	0.3
S2 Plateau	5.83	10.33	28.83	28.17	8.33	4.41
S2 Observed	5	7.5	25	21	7.5	4
S3 Jump	0.41	5.82	49.25	68.16	7.83	0.75
S3 Plateau	8.16	20.16	61.83	74.42	8.5	27
S3 Observed	9	15	53	68	9.33	27

*Note that sensor jump, plateau, and observed times are reported in minutes

Oxygen can only penetrate a few millimeters or centimeters into the bed sediment before it is depleted (Precht *et al*. 2004, Glud 2008). In less permeable soils that allow shorter penetration depths, the jump, plateau, and exposure times practically coincide. As permeability increases and oxygen penetration depths extend, the plateau times serve as a better representation of when the observed maximum scour depth reaches the sensor location. This is because the small spacing between adjacent sensors in these scaled experiments is comparable to the oxygen penetration depths in more permeable soils. Should these sensors be deployed on a real bridge, the spacing should be large enough that the time interval between the jump and plateau will be negligible compared to the time it takes for the scour hole to extend from one sensor location to the next.

Although the output signal is independent of changes in flow velocity, larger velocities could lead to faster response times of the sensors. Thus, steady-state DO levels were achieved more quickly for sensors closer to the soil bed, which were also exposed to larger flow velocities. Also, during some stages of scour hole evolution, the vortices around the pier (see Fig. 5(b)) caused the sensor closest to the scoured bed surface to cycle through semi-buried to exposed conditions for some time before becoming completely exposed. These rapid undulations from anoxic or suboxic bed sediment to oxic water caused the signal to show an initial gradual increase in DO levels before rising to steady-state DO levels at full exposure, because the 5 s measurement interval (as limited by the data acquisition system's sampling rate) was not enough time for capturing these changes more accurately. This effect was observed for sensors buried deeper (e.g., see DO levels at S3 in Fig. 10).

A similar observation was made while performing scour tests with the Russian River sand (i.e., Test #6 of Table 1). As indicated by the particle size distribution in Fig. 4, this soil contained fine gravel and coarse sands in addition to the finer sandy material. According to Allen (1965), when the streambed has a wide range of particle sizes, the finer particles would be transported in suspension, while coarser particles tend to roll or move on or near the bed. This phenomenon was observed in the case of the Russian River sand in that the finer grains scoured very quickly, causing a jump in the DO level at the sensor closest to the surface, while the larger particles remained around the pier for a longer time before they too were transported away. These larger

particles intermittently blocked the sensors, which led to longer time gaps between the jump and plateau times. The plateau in DO levels occurred almost exactly when the larger grains were washed away and when the sensor tip was fully exposed.

3.3 Effects of scour hole refill

Tidal cycles and changes in flow direction may cause some backfilling around bridge piers or abutments and effectively retard or even reverse the scour process. The DO sensors could also detect refilling of the scour hole, as demonstrated in Fig. 12. Fig. 12 shows a scour hole refill test conducted as part of Test #3 (i.e., soil with 35% silica as shown in Table 1). After S3 had been exposed by the original scour test, the flow rate was decreased to a level insufficient to mobilize sediments. Then, the scour hole was refilled by manually packing the eroded soil back into the hole, followed by leveling the surface so that all the sensors were once again embedded at their original depths.

The refill resulted in a gradual decrease in DO levels as shown by the DO levels for S1, S2, and S3 in Fig. 12. After ~85 min, the flow rate was increased to the 0.35 m/s velocity range to promote another round of scour development (which began at time 0 as shown in Fig. 12). However, during this experiment, some segregation occurred during the backfilling process, and silica levels were reduced from ~35% at the bottom to almost 0% at the final bed level. This was the reason why the DO levels were reduced to different levels during the allotted time between refill and re-scour. Also, because the refilled material was of a lower permeability, the subsequent scouring occurred faster, and the sensors' exposure times were closer to each other. S2 was exposed within only 30 s of S1, which is why the sensor symbols for the first two exposure conditions appear to be overlapped in Fig. 12.

The experimental results were promising in that they demonstrated the possibility of using DO sensors for determining the maximum scour depth around a bridge pier. Since the sensors were located at discrete locations along the height of the pier, the detection resolution would depend on the spacing between adjacent sensors, which would in turn be determined based on the bed sediment permeability and the resolution requirements of the parent structural health monitoring system.

3.4 Comparison with current established monitoring methods

Scour monitoring using DO probes offers many appealing advantages as compared to other existing or emerging techniques. For example, sonar (De Falco and Mele 2002), radar (Millard *et al.* 1998), and TDR (Yankielun and Zabilansky 1999) sensing devices measure scour depth by correlating the time it takes for an emitted pulse to travel to and reflect from the scoured bed surface. The main drawback in these devices is that signal analysis can be quite challenging and susceptible to complications resulting from debris, turbidity, or turbulence interferences. The DO sensing method proposed in this study does involve fairly complex signal analysis, but it is not as sensitive to interferences due to its miniature size and the fact that the signal travels only a short distance. Also, the results from DO measurements provide a binary assessment of whether scour has occurred or not, and hence, are extremely straightforward. Another group of sensors includes devices like accelerometers (Briaud *et al.* 2011) and tilt sensors (Yao *et al*. 2010). These sensors are typically mounted on the superstructure, and their measurement of scour is indirect, as the techniques they use often involve using vibration measurements that may be from sources not

related to scour. In contrast, DO sensors provide a direct indication of sediment transport.

One of the simplest scour sensing devices is the aptly named float-out sensor (Lueker *et al*. 2010), which transmits a signal once it floats out from the initial buried position due to scour. These devices are difficult to install, and since they float out, their application is limited to one scour event at a time. Installation of new float-out sensors after every scour event adds to the infrastructure operating and maintenance costs. In contrast, as seen from the results of this study, DO sensors were capable of detecting numerous cycles of scour and backfill. On the other hand, scour monitoring devices involving fiber optics (Lin *et al.* 2005), piezoelectrics (Azhari *et al*. 2014), MEMS (Lin *et al*. 2010), and switches (Liu *et al*. 2010) all use mechanically intensive techniques in one way or another, which make them particularly vulnerable to debris as they are typically installed along a rod-like structure that is required to have a range of motion. DO sensors, instead, can be compactly mounted along the pier itself, eliminating any damage imposed by large tree branches and other debris carried by the fast moving waters during a flood. It should be noted, however, that considering the sensing mechanism, DO scour sensors may not be effective in eutrophic or extremely turbid waters. Further tests are required to examine the efficiency of DO sensors in these conditions.

3.5 Future research

The extent of vertical advection of pore water through the surface sediment layer of the scour hole affects degree of DO depletion and the maximum possible resolution offered by DO sensors. Sediments with higher permeability allow more pore water flow, leading to deeper oxygen penetration and a more complicated oxygen dynamics at the soil-water interface. Additional research can determine any potential complications caused by changes in permeability, especially in stratified riverbeds or in situations where soil disturbance causes the boundary flow to change the oxygen gradients within the upper sediment layer.

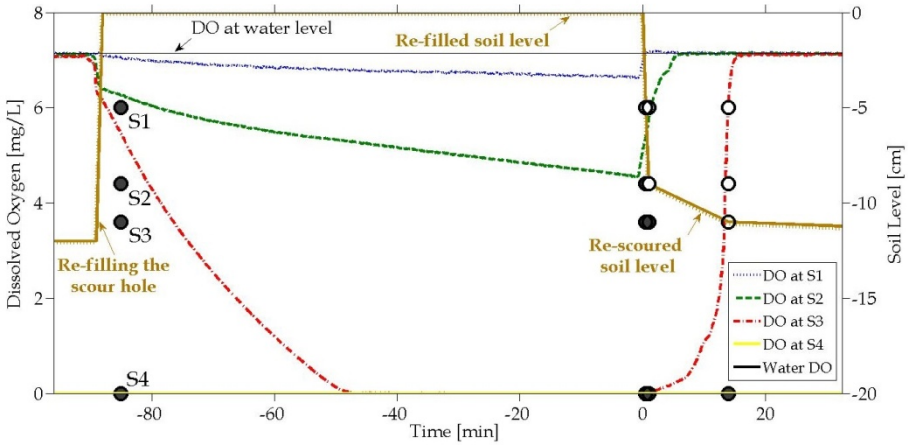

Fig. 12 Refill and re-scour response for the “35% Silica + 65% Well-Pack Sand” soil type are shown. The filled and open circles indicate buried and exposed DO probes, respectively

Lastly, as mentioned in a study by Sumer (2007), the upward directed pore water pressure gradients during tsunamis can lead to very deep scour holes at piles, resulting from the very quick and transient scour enhanced by the loss of soil effective stress. DO probes can potentially detect any increase in pore pressure by monitoring the soils' oxygen levels. This would mean that these sensors can be used to detect the initiation of scour around bridge foundations and other hydraulic structures, such as wind turbines and breakwaters, induced by tsunamis or momentary liquefaction (Tonkin *et al*. 2003, Sumer 2007). The same analogy can be applied to use DO sensors for detecting the initiation of internal erosion and piping problems in dams (Fell *et al*. 2003). These are new avenues that can be explored as part of future research on the use of DO sensors for structural health monitoring.

4. Conclusions

The problem of scour-induced failure or loss of capacity can be eliminated through the implantation of real-time scour monitoring systems on overwater bridges and other hydraulic structures. The results from this study provide a preliminary proof-of-concept for the use of oxygen sensing optodes to detect maximum local scour depth at bridge piers. These sensors offer clear advantages over other scour sensing technologies in that they are mechanically robust, provide a straightforward binary response to scour, and are less susceptible to debris, turbulence, and other interferences.

Laboratory flume experiments were conducted in which miniature DO probes were embedded at four locations along the buried length of a simulated circular bridge pier, facing upstream. Scour around the pier exposed the top three sensors one by one. As each sensor emerged from beneath the sediments, DO measurements increased abruptly to values comparable to the oxygen content in flowing water. The time at which a surge in DO response occurred was indicative of the emergence of the corresponding sensor, which in turn meant that the scour hole had reached a maximum depth equivalent to that of the sensor. Through scour experiments on six different soil mixtures, the dependence of permeability on the time lag between the signal jump and steady-state conditions was investigated; the lower the permeability, the shorter the lag. For highly permeable sediments, the time at which DO levels reached the steady-state plateau was found to be a better representation of the scour hole actually reaching the sensor depth. Furthermore, these sensors were capable of detecting subsequent scour after the scour hole was refilled.

Further research is required to examine the repeatability of these results through comprehensive laboratory and field tests on various soils with different levels of vertical advection. Temperature was found to have a significant effect on DO values; therefore, future applications of this sensing system must involve simultaneous in situ temperature measurements. Also, the dependence of DO levels on water salinity, aquatic life forms, and common spatial or temporal aerobic activities and metabolic processes in marine sediments should be explored to ascertain whether further calibration and corrections are necessary.

Acknowledgments

The authors gratefully acknowledge support from the U.S. National Science Foundation (NSF grant no. CMMI-1234080). Additional support was provided by the American Society of Civil

Engineers (ASCE) Freeman Fellowship and the College of Engineering, University of California, Davis. PreSens and Prof. Jason DeJong are also recognized for their assistance. The authors also acknowledge Prof. Fabian Bombardelli for his collaboration.

References

Allen, J.R.L. (1965), "A review of the origin and characteristics of recent alluvial sediments", *Sedimentology*, **5**(2), 89-191.

Apsilidis, N., Diplas, P., Dancey, C., Vlachos, P. and Raben, S. (2010), "Local scour at bridge piers: the role of Reynolds number on horseshoe vortex dynamics", *Proceedings of the 5th International Conference on Scour and Erosion (ICSE-5)*, San Francisco, USA, November.

ASTM Standard D2487 (2011), *Standard Practice for Classification of Soils for Engineering Purposes (Unified Soil Classification System)*, ASTM International, West Conshohocken, PA, USA.

ASTM Standard D421-85 (2007), *Standard Practice for Dry Preparation of Soil Samples for Particle-Size Analysis and Determination of Soil Constants*, ASTM International, West Conshohocken, PA, USA.

Azhari, F., Tom, C., Benassini, J., Loh, K.J. and Bombardelli, F.A. (2014), "Design and characterization of a piezoelectric sensor for monitoring scour hole evolution", *Proceedings of SPIE Smart Structures/NDE Conference*, San Diego, USA, March.

Benedict, S., Deshpande, N. and Aziz, N. (2007), "Evaluation of abutment scour prediction equations with field data", *Transportation Research Record: J. Transportation Research Board*, **2025**(1), 118-126.

Briaud, J.L., Hurlebaus, S., Chang, K.A., Yao, C., Sharma, H., Yu, O.Y., Darby, C., Hunt, B.E. and Price, G.R. (2011), *Realtime monitoring of bridge scour using remote monitoring technology*, Texas Transportation Institute, Texas A&M University System.

Briaud, J.L., Ting, F.C.K., Chen, H.C., Cao, Y., Han, S.W. and Kwak, K.W. (2001), "Erosion function apparatus for scour rate predictions", *J. Geotech. Geoenviron.*, **127**(2), 105-113.

Butch, G.K. (1996), "Scour-hole dimensions at selected bridge piers in New York", *North American Water and Environment Congress & Destructive Water, ASCE*, Anaheim, USA, June.

Calver, A. (2001), "Riverbed permeabilities: information from pooled data", *Ground Water*, **39**(4), 546-553.

Chen, G., Pommerenke, D. and Zheng, R. (2011), *Smart rocks and wireless communication systems for real-time monitoring and mitigation of bridge scour*, Missouri University of Science and Technology.

Choi, S.U. and Cheong, S. (2006), "Prediction of local scour around bridge piers using artificial neural networks", *JAWRA Journal of the American Water Resources Association*, **42**(2), 487-494.

Dargahi, B. (1990), "Controlling mechanism of local scouring", *J. Hydraul. Eng.*, **116**(10), 1197-1214.

Dat, J.F., Capelli, N., Folzer, H., Bourgeade, P. and Badot, P.M. (2004), "Sensing and signalling during plant flooding", *Plant Physiology and Biochemistry*, **42**(4), 273-282.

De Falco, F. and Mele, R. (2002), "The monitoring of bridges for scour by sonar and sedimetri", *NDT & E Int.*, **35**(2), 117-123.

Deng, L. and Cai, C. (2010), "Bridge scour: prediction, modeling, monitoring, and countermeasures-review", *Practice Periodical on Struct. Des. Constr.*, **15**(2), 125-134.

Ebbert, J.C. (2002), *Concentrations of Dissolved Oxygen in the Lower Puyallup and White Rivers, Washington, August and September 2000 and 2001*, U.S. Dept. of the Interior, U.S. Geological Survey, Tacoma, WA, USA.

Fell, R., Wan, C., Cyganiewicz, J. and Foster, M. (2003), "Time for development of internal erosion and piping in embankment dams", *J. Geotech. Geoenviron.*, **129**(4), 307-314.

Glud, R.N. (2008), "Oxygen dynamics of marine sediments", *Marine Biology Research*, **4**(4), 243-289.

Govindasamy, A., Briaud, J., Kim, D., Olivera, F., Gardoni, P. and Delphia, J. (2013), "Observation method for estimating future scour depth at existing bridges", *J. Geotech. Geoenviron.*, **139**(7), 1165-1175.

Hazen, A. (1892), *Some physical properties of sands and gravels: with special reference to their use in filtration*, Massachusetts State Board of Health, 24th Annual Report.

Hazen, A. (1911), "Discussion of 'Dams on sand foundations' by A. C. Koenig", *Trans. Am. Soc. Civ. Eng.*, **73**, 199-203.
Hong, J., Chiew, Y., Lu, J., Lai, J. and Lin, Y. (2012), "Houfeng bridge failure in Taiwan", *J. Hydraul. Eng. -ASCE*, **138**(2), 186-198.
Hunt, B.E. (2005), *Practices for monitoring scour critical bridges*, NCHRP Project, First Draft Report.
John, G.T. and Huber, C. (2005), *Instruction Manual OXY-4,* PreSens Precision Sensing GmbH, Regensburg, Germany.
Johnson, P. (1995), "Comparison of pier-scour equations using field data", *J. Hydraul. Eng. -ASCE,* **121**(8), 626-629.
Klimant, I., Kühl, M., Glud, R.N. and Holst, G. (1997), "Optical measurement of oxygen and temperature in microscale: strategies and biological applications", *Sensor. Actuat. B - Chem.* **38**(1-3), 29-37.
Klimant, I., Meyer, V. and Kühl, M. (1995), "Fiber-optic oxygen microsensors, a new tool in aquatic biology", *Limnol. Oceanogr.*, **40**(6), 1159-1165.
Klimant, I. and Wolfbeis, O.S. (1995), "Oxygen-sensitive luminescent materials based on silicone-soluble ruthenium diimine complexes", *Anal. Chem.*, **67**(18), 3160-3166.
Kondolf, G.M., Williams, J.G., Horner, T.C. and Milan, D. (2008), "Assessing physical quality of spawning habitat", *American Fisheries Society Symposium,* **65**, 249-274.
Koski, K.V. (1966), *The survival of coho salmon (Oncorhynchus kisutch) from egg deposition to emergence in three Oregon coastal streams*, M.S. Dissertation, Oregon State University, Oregon.
Lin, Y.B., Chen, J.C., Chang, K.C., Chern, J.C. and Lai, J.S. (2005), "Real-time monitoring of local scour by using fiber bragg grating sensors", *Smart Mater. Struct.*, **14**(4), 664-670.
Lin, Y.B., Lai, J.S., Chang, K.C., Chang, W.Y., Lee, F.Z. and Tan, Y.C. (2010), "Using MEMS sensors in the bridge scour monitoring system", *J. Chinese Inst. Engineers*, **33**(1), 25-35.
Liu, Y.T., Tong, J.H., Lin, Y., Lee, T.H. and Chang, C.F. (2010), "Real-time bridge scouring safety monitoring system by using mobile wireless technology", *Proceedings of the 4th International Conference on Genetic and Evolutionary Computing (ICGEC)*, Shenzhen, China, IEEE.
Lueker, M., Marr, J., Ellis, C., Hendrickson, A. and Winsted, V. (2010). "Bridge scour monitoring technologies: development of evaluation and selection protocols for application on river bridges in Minnesota", *Proceedings of the 5th International Conference on Scour and Erosion (ICSE-5)*, San Francisco, USA, November.
Melville, B.W. and Coleman, S.E. (2000), *Bridge scour*, Water Resources Publication, CO, USA.
Melville, B.W. and Raudkivi, A.J. (1996), "Effects of foundation geometry on bridge pier scour", *J. Hydraulic Eng,*, **122**(4), 203-209.
Millard, S.G., Bungey, J.H., Thomas, C., Soutsos, M.N., Shaw, M.R. and Patterson, A. (1998), "Assessing bridge pier scour by radar", *NDT & E Int.*, **31**(4), 251-258.
Minard, C.J. (1856), *De la chute des ponts dans les grandes crues*, Collections de l'École nationale des ponts et chaussées, Paris, France.
Park, I., Lee, J. and Cho, W. (2004). "Assessment of bridge scour and riverbed variation by a ground penetrating radar", *Proceedings of the 10th International Conference on Ground Penetrating Radar (GPR 2004)*, Delft, The Netherlands, IEEE, **1**, 411-414.
Parsons, R.L., Bennett, C., Han, J. and Lin, C. (2014), *Case history analysis of bridge failures due to scour*, Climate Effects on Pavement and Geotechnical Infrastructure, ASCE Publications.
Precht, E., Franke, U., Polerecky, L. and Huettel, M. (2004), "Oxygen dynamics in permeable sediments with wave-driven pore water exchange", *Limnol. Oceanogr.*, **49**(3), 693-705.
Richardson, J.R., Price, G.R., Richardson, E.V. and Lagasse, P.F. (1996), *Modular magnetic scour monitoring device and method for using the same*, U.S. Patent No. 5,532,687, Washington, DC: U.S. Patent and Trademark Office, USA.
Shirazi, M.A. and Seim, W.K. (1981), "Stream system evaluation with emphasis on spawning habitat for salmonids", *Water Resour. Res.*, **17**(3), 592-594.
Soulsby, R. (1997), *Dynamics of marine sands a manual for practical applications*, Telford, London.
Stern, O. and Volmer, M. (1919), "Über die abklingungszeit der fluoreszenz", *Physikalische Zeitschrift*, **20**,

183-188.
Sumer, B.M. (2007), "Mathematical modelling of scour: a review", *J. Hydraul. Res.*, **45**(6), 723-735.
Tonkin, S., Yeh, H., Kato, F. and Sato, S. (2003), "Tsunami scour around a cylinder", *J. Fluid Mech.*, **496**, 165-192.
van Rijn, L. (1984), "Sediment transport, part III: bed forms and alluvial roughness", *J. Hydraul. Eng,*, **110**(12), 1733-1754.
White, K. (1992), *Bridge maintenance inspection and evaluation*, (2nd Ed.), CRC Press, USA.
Wingrove, J. (2013), *Train cars carrying petroleum products safely removed from partially collapsed Calgary bridge*, The Globe and Mail, June.
Xiong, W., Cai, C.S. and Kong, X. (2012), "Instrumentation design for bridge scour monitoring using fiber bragg grating sensors", *Appl. Optics*, **51**(5), 547-557.
Yankielun, N. and Zabilansky, L. (1999), "Laboratory investigation of time-domain reflectometry system for monitoring bridge scour", *J. Hydraul. Eng.*, **125**(12), 1279-1284.
Yao, C., Darby, C., Hurlebaus, S., Price, G., Sharma, H., Hunt, B., Yu, O., Chang, K. and Briaud, J. (2010), "Scour monitoring development for two bridges in Texas", *Proceedings of the 5th International Conference on Scour and Erosion (ICSE-5)*, San Francisco, USA, November.
Yu, X. and Yu, X. (2010), *Field Monitoring of Scour Critical Bridges: A Pilot Study of Time Domain Reflectometry Real Time Automatic Bridge Scour Monitoring System*, Ohio Department of Transportation, Ohio, USA.
Yu, X. and Zabilansky, L. (2010). "Time domain reflectometry for automatic bridge scour monitoring", *Site and Geomaterial Characterization*, Shanghai, China.
Zhou, Z., Huang, M., Huang, L., Ou, J. and Chen, G. (2011), "An optical fiber bragg grating sensing system for scour monitoring", *Adv. Struct. Eng.*, **14**(1), 67-78.